The Journal of Immunology

Recapitulation of Normal and Abnormal BioBreeding Rat T Cell Development in Adult Thymus Organ Culture

Barbara J. Whalen, Peter Weiser, Jan Marounek, Aldo A. Rossini, John P. Mordes and Dale L. Greiner

J Immunol 1999; 162:4003-4012; ;
http://www.jimmunol.org/content/162/7/4003

The Journal of Immunology is published twice each month by
The American Association of Immunologists, Inc.,
1451 Rockville Pike, Suite 650, Rockville, MD 20852

Print ISSN: 0022-1767 Online ISSN: 1550-6606.

Recapitulation of Normal and Abnormal BioBreeding Rat T Cell Development in Adult Thymus Organ Culture[1]

Barbara J. Whalen, Peter Weiser, Jan Marounek, Aldo A. Rossini, John P. Mordes, and Dale L. Greiner[2]

Congenitally lymphopenic diabetes-prone (DP) BioBreeding (BB) rats develop spontaneous T cell-dependent autoimmunity. Coisogenic diabetes-resistant (DR) BB rats are not lymphopenic and are free of spontaneous autoimmune disease, but become diabetic in response to depletion of RT6$^+$ T cells. The basis for the predisposition to autoimmunity in BB rats is unknown. Abnormal T cell development in DP-BB rats can be detected intrathymically, and thymocytes from DR-BB rats adoptively transfer diabetes. The mechanisms underlying these T cell developmental abnormalities are not known. To study these processes, we established adult thymus organ cultures (ATOC). We report that cultured DR- and DP-BB rat thymi generate mature CD4 and CD8 single-positive cells with up-regulated TCRs. DR-BB rat cultures also generate T cells that express RT6. In contrast, DP-BB rat cultures generate fewer CD4$^+$, CD8$^+$, and RT6$^+$ T cells. Analysis of the cells obtained from ATOC suggested that the failure of cultured DP-BB rat thymi to generate T cells with a mature phenotype is due in part to an increased rate of apoptosis. Consistent with this inference, we observed that addition of the general caspase inhibitor Z-VAD-FMK substantially increases the number of both mature and immature T cells produced by DP-BB rat ATOC. We conclude that cultured DR-BB and DP-BB rat thymi, respectively, recapitulate the normal and abnormal T cell developmental kinetics and phenotypes observed in these animals in vivo. Such cultures should facilitate identification of the underlying pathological processes that lead to immune dysfunction and autoimmunity in BB rats. ***The Journal of Immunology,*** **1999, 162: 4003–4012.**

BioBreeding (BB)[3] rats are susceptible to spontaneous autoimmune hyperglycemia and are used to model human insulin-dependent diabetes mellitus (IDDM) (1–3). Two lines of inbred BB rats have been developed for parallel study of susceptibility and resistance to disease. The cumulative incidence of spontaneous hyperglycemia in the diabetes-prone (DP) BB rat is >90% (4). Diabetes-resistant (DR) BB rats were derived from DP forebears, but after breeding for resistance their cumulative incidence of spontaneous diabetes is 0% (4). Diabetes in the DP-BB rat is T cell dependent, and spleen cells from diabetic animals adoptively transfer the disease (1–3). Insulitis (selective destruction of pancreatic islet β cells) is observed in all affected animals (1).

DP-BB rats have severe T cell lymphopenia (5–9), an abnormality not found in humans with IDDM. T cell subsets present in abnormally low numbers in DP-BB rats include those expressing CD8 (10), RT6 (11), and to a lesser extent CD4 (5). DR-BB rats do not share the lymphopenia of DP animals and have a normal distribution of T cell subsets (11). An autosomal recessive locus, *lyp*, determines the T cell lymphopenia (12–14). Lymphopenia and diabetes susceptibility can be independently inherited traits (15, 16), but deficiency in peripheral T cells appears to be tightly linked with the expression of spontaneous IDDM in BB rats (13, 14, 17, 18).

In vivo developmental studies have documented that the abnormal T cell maturation in DP-BB rats due to *lyp* can be detected intrathymically (19, 20). The defect also affects recent thymic emigrants, naive peripheral T cells (21, 22), and intraepithelial lymphocytes (23, 24). The mechanisms by which the *lyp* gene affects T cell development remain unknown, in part due to the difficulty of analyzing its intrathymic actions in vivo. To investigate the cell biology of this process in the rat, we have established adult thymus organ cultures (ATOC). We report that cultured DR- and DP-BB thymus fragments, respectively, recapitulate the normal and abnormal T cell development that is observed in these animals in vivo.

Materials and Methods

Animals

Viral Ab-free DP-BB and DR-BB rats were purchased from the colony at the University of Massachusetts Medical Center (Worcester, MA). They were certified as free of Sendai virus, pneumonia virus of mice, sialodacryoadenitis virus, rat corona virus, Kilham rat virus, H1 (Toolan's virus), GD7, Reo-3, *Mycoplasma pulmonis*, lymphocytic choriomeningitis virus, mouse adenovirus, Hantaan virus, and *Encephalitozoon cuniculi*. They were maintained in accordance with the *Guide for the Care and Use of Laboratory Animals* (Institute of Laboratory Animal Resources, National Research Council, National Academy of Sciences, 1996).

ATOC

Thymi were obtained from adult male or female BB rats 55–66 days of age. Thymi were rinsed three times in sterile HEPES-buffered RPMI 1640 without sodium bicarbonate (H-RPMI). Adherent lymph nodes and fatty tissue were removed. Thymi were placed onto a microscope slide and were

Diabetes Division, University of Massachusetts Medical Center, Worcester, MA

Received for publication June 18, 1998. Accepted for publication January 4, 1999.

The costs of publication of this article were defrayed in part by the payment of page charges. This article must therefore be hereby marked *advertisement* in accordance with 18 U.S.C. Section 1734 solely to indicate this fact.

[1] This work was supported in part by Grants DK25306 (A.A.R.), DK36024 (D.L.G.), and DK41235 (J.P.M.) from the National Institutes of Health, an institutional Diabetes and Endocrinology Research Center Grant from the National Institutes of Health, and by a Career Development Award from the Juvenile Diabetes Foundation International (B.J.W.). The contents of this publication are solely the responsibility of the authors and do not necessarily represent the official views of the National Institutes of Health.

[2] Address correspondence and reprint requests to Dr. Dale L. Greiner, Diabetes Division, University of Massachusetts Medical School, Two Biotech, 373 Plantation Street, Suite 218, Worcester, MA 01605. E-mail address: Dale.Greiner@umassmed.edu

[3] Abbreviations used in this paper: BB, BioBreeding; ATOC, adult thymic organ culture; BrdU, bromodeoxyuridine; DP, diabetes-prone; DR, diabetes-resistant; IDDM, insulin-dependent diabetes mellitus; H-RPMI, HEPES-buffered RPMI; PE, phycoerythrin; TUNEL, terminal deoxynucleotidyl transferase-mediated dUTP-nick end labeling; FTOC, fetal thymic organ culture.

0022-1767/99/$02.00

cut vertically into eight strips. Thymus strips were moistened with a solution of H-RPMI plus 10% FBS (HyClone, Logan, UT) and kept on ice. Very fine forceps and dissecting scissors were used to cut the thymus strips into 1-mm^3 fragments.

Thymus fragments were cultured on filters (0.45 μm HAWP04700 filters, Millipore, Bedford, MA) placed on top of 2 × 6 cm Gelfoam sponges (Upjohn, Kalamazoo, MI). Each Gelfoam sponge was hydrated overnight in a 100 × 25-mm tissue culture dish containing 10 ml HEPES-buffered DMEM with sodium pyruvate (high glucose formulation) supplemented with 100 U/ml penicillin, 0.1 mg/ml streptomycin, 125 ng/ml gentamicin, 2 mM glutamine, 1× nonessential amino acids, 5×10^{-5} M 2-ME, and 20% heat-inactivated FBS (HyClone). Thymus fragments were cultured in petri dishes in a humidified incubator in an atmosphere of 7% CO_2 and air at 37°C. Each thymus lobe was divided in two, and each half was cultured separately. Cultures were fed on day 7 with 5 ml of supplemented HEPES-buffered DMEM; cultures were maintained for a maximum of 15 days. Sterile technique was used throughout. At the time of cell harvest, the two cultures comprising one thymus lobe were recombined and analyzed together, except in experiments involving culture in the presence of Z-VAD-FMK (see below).

For harvesting, filters were removed from the cultures, cut in half, and placed tissue side down in sterile 6-well tissue culture dishes containing 3 ml of collagenase solution in sodium phosphate buffer with 0.2 mg/ml disodium EDTA, pH 7.4. Collagenase solutions were prepared just before use with 0.4 mg/ml of collagenase from *Clostridium histolyticum* Type IV (Sigma, St. Louis, MO) and sterile filtered before use. Tissues were digested for 30 min at 37°C. Digestion was stopped by placing the plates on ice and by adding 0.5 ml of FBS (HyClone) to each well. Thymus fragments were picked from the filters and placed into H-RPMI medium. Residual thymus tissue was flushed off of the filters by pipetting. Thymus fragments were gently extruded through a cell sieve (50-mesh screen), filtered through a 70-μm sterile cell strainer (Falcon #2350), and washed twice in H-RPMI. Viable cell number was determined by trypan blue dye exclusion using a hemocytometer.

In certain experiments, the caspase inhibitor Z-VAD-FMK (Enzyme Systems Products, Livermore, CA) was reconstituted according to manufacturer's instructions immediately before use and added to cultures on day 0. In these experiments, data analysis was performed on the cells generated by each individually cultured half-thymus lobe.

Design of kinetic studies

Cells from an individual thymus culture plate (i.e., one half-thymus lobe) could be harvested only once, and for that reason repetitive sampling was not possible. To perform kinetic analyses, individual cultures were established for each time point of interest. A minimum of eight individual cultures, each representing one half of a thymus lobe, were established for analysis of each time point during culture. Each data point in Fig. 1 represents the mean ± SD for 4–12 entire thymus lobes at each time point. Cell counts are expressed as total cells recovered per individual thymic lobe.

Flow cytometric analysis

Single- and dual-color flow microfluorometry was used to quantify the expression of cell surface markers (25). Abs to the TCR-$\alpha\beta$ (clone R73), IL-2R α-chain (clone OX-39), CD4 (clone OX-35), CD8 α-chain (clone OX-8), and Thy-1.1 (clone OX-7) were purchased from PharMingen (San Diego, CA). Hybridoma-secreting anti-RT6.1 (clone DS4.23) is maintained in our laboratory. Isotype control FITC-conjugated mouse IgG1 and biotin-conjugated mouse IgG1, mouse IgG2a, and rat IgG2b were also purchased from PharMingen, as was phycoerythrin (PE)-conjugated streptavidin. Biotin-conjugated anti-RT6.1 (rat IgG2b isotype) was prepared from affinity-purified DS4.23 using BIOTIN-X-NHS (Calbiochem, La Jolla, CA). All Abs except anti-Thy-1.1 were used at a concentration of 1 μg per 10^6 cells. Anti-Thy-1.1 Abs were used at a concentration of 0.5 μg per 10^6 cells due to intense labeling of thymocytes and immature T cells. PE-conjugated streptavidin was used at a concentration of 0.5 μg per 10^6 cells. Samples were fixed in a final concentration of 1% paraformaldehyde in PBS and analyzed using a FACScan. A minimum of 7500 viable cells in each sample was analyzed. The lymphocyte fraction was gated on the basis of forward and side scatter. Results are presented as the percentage of positive cells in the lymphocyte fraction of the cultures with background isotype control values subtracted.

Three-color flow microfluorometry was used for analyses of cell proliferation and certain TUNEL assays. ATOC were pulsed for 16–17 h before harvest with bromodeoxyuridine (BrdU) at a final concentration of 25 μg/ml. As a positive control, P815 tumor cells were pulsed in vitro for 3–4 h with BrdU at the same concentration. Cultures were harvested and

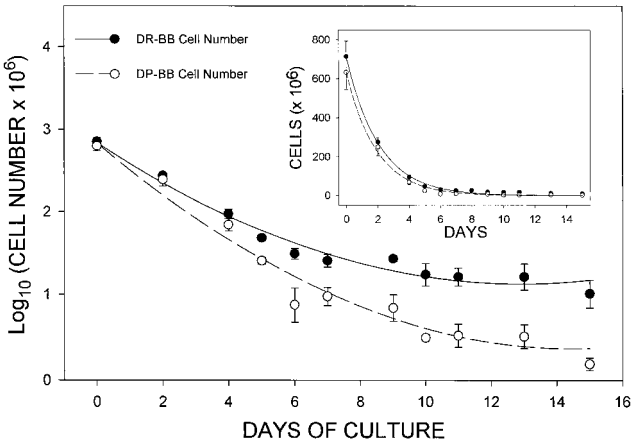

FIGURE 1. Number of viable cells recovered from DR- and DP-BB rat ATOC over time. Cultures were established as described in *Materials and Methods*. Each data point represents mean ± 1 SD of the $\log_{10}$ (viable cell number) of 4–11 thymic lobes at each time point. Each data point was obtained from an independent culture; cultures were not counted repetitively over time. The inset graph shows the data plotted linearly and fitted by first-order nonlinear regression. In the main graph, the data are plotted on a log-linear scale to illustrate the differences between DP and DR ATOC at later time points; these data were fitted by second-order linear regression. For DR ATOC, $\log_{10}$ (cell number) = $2.837 - 0.26t + 0.010t2$, $r^2 = 0.94$. For DP ATOC, $\log_{10}$ (cell number) = $2.833 - 0.34t + 0.012t2$, $r^2 = 0.96$.

surface labeled with PE- and biotin-conjugated mAbs followed by Cy Chrome-conjugated streptavidin (PharMingen). Cells were fixed, permeabilized, treated with DNase (Sigma), and labeled with FITC-conjugated anti-BrdU mAb (Becton Dickinson, San Jose, CA) as described (26). Negative control ATOC were incubated in the absence of BrdU, processed as above, and labeled with FITC-conjugated anti-BrdU mAb.

Apoptotic cells were detected by flow microfluorometry using a fluorescein-based in situ detection kit (TUNEL assay, Boehringer Mannheim, Indianapolis, IN). The average background in samples not treated with terminal deoxynucleotidyl transferase was only 1.3%, and this value was not subtracted from experimental readings. TUNEL$^+$ T cell subsets were analyzed by three-color staining. Cells were first labeled with PE- or biotin-conjugated Abs, then incubated with Cy Chrome-streptavidin, fixed, and stained for TUNEL$^+$ cells according to manufacturer's directions.

With one exception, all analyses of BrdU$^+$ and TUNEL$^+$ cells were gated on the viable lymphocyte fraction as determined by forward and side light scatter characteristics. The single exception was a TUNEL assay of total nucleated cells (see Fig. 4*A*). A minimum of 25,000 events were analyzed in triple-staining analyses.

Morphology

Thick sections of intact cultured thymic fragments still attached to filters were prepared by fixation in Bouin's solution for 6 h. Fixed specimens were washed overnight, embedded in paraffin, cut into 5-μm sections, stained with hematoxylin and eosin, and examined by light microscopy. Thin sections of intact cultured thymic fragments still attached to filters were prepared by fixation for 2 h in 3% glutaraldehyde in cacodylate buffer at pH 7.4, rinsed three times in buffer, fixed in 2% osmium tetroxide for 2 h, and rinsed four times in buffer. This procedure dissolved the filter. Fixed specimens were dehydrated and embedded in 1:1 propylene oxide and epoxy resin. Sections 1.5 μm thick were mounted on glass slides and stained with 0.5% toluidine blue. Slides mounted in Permount were examined using a Nikon Eclipse E600 microscope and a Nikon Plan Fluor objectives (Tokyo, Japan). Images were captured using a SPOT color digital camera (Diagnostic Instruments, Sterling Heights, MI).

Statistics

Data are summarized as arithmetic means ± SD. Because thymic organ cultures were not sampled repetitively over time, the number and percentage of cells present at different time points is compared with the average number of cells recovered from uncultured thymic lobes. In experiments

involving culture in the presence of varying concentrations of caspase inhibitor, only one time point was used; the number and percentage of cells present at different concentrations of inhibitor represents the mean of three individual half-thymus lobe cultures. Curve fitting was performed using SigmaPlot software (ver. 4.0, SPSS, Chicago, IL). Comparisons of three or more means used one-way analysis of variance and the least significant difference procedure for a posteriori contrasts (27). Comparisons of two means used Student's *t* test with separate variance estimates (27). Where appropriate, correction for multiple comparisons was made using the Bonferroni adjustment (28).

Results

ATOC yields larger numbers of DR- than DP-BB rat thymocytes

The number of viable cells recovered from DR- and DP-BB rat ATOC at various time points is shown in Fig. 1. The number of cells recovered from each freshly isolated DR-BB rat thymus averaged 714 ± 79 × 10^6 per lobe (n = 8). The number recovered from freshly isolated DP-BB rat thymus was somewhat lower, 640 ± 93 × 10^6 per lobe (n = 9), but the difference between the two strains was not statistically significant (p = 0.60). The number of cells recovered declined progressively over the 15-day period of culture. The greatest decline in cell number occurred during the first 4 days, during which ~90% of cells were lost. In comparison with the average number of cells present in freshly isolated thymi, only 13.2 ± 1.8% of DR- (n = 4) and 10.9 ± 1.8% of DP-BB (n = 4) thymocytes remained after 4 days of culture. The magnitudes of cell loss in DR- and DP-BB rat ATOC on day 4 were statistically similar (p = 0.78). By day 15, only 1.2 ± 0.7% of DR-BB (n = 8) and 0.2 ± 0.04% of DP-BB (n = 4) cells remained; this difference between DR- and DP-BB rat ATOC cell recovery was statistically significant (p = 0.006).

Inspection of both DR- and DP-BB rat ATOC kinetics suggested that cell number over time was determined predominantly by cell death. Consistent with this inference, the decline in cell number over time exhibited first order exponential decay kinetics (Fig. 1, inset). The calculated half-life of DR cells in ATOC was 1.43 days, and the half-life of DP-BB cells was 1.32 days.

However, first-order exponential decay did not fully describe the behavior of ATOC at later time points, notably after day 5. This observation suggested that cell proliferation rates also played a role in determining cell number over time. To test this hypothesis quantitatively, the data were refitted using second order regression. As shown in Fig. 1, the decline in cell number did appear closely to follow second order kinetics. The coefficients associated with the first-order term (cell death) were different for DR (−0.26) and DP (−0.34) ATOC, whereas the second-order terms (cell proliferation) were similar for DR (+0.010) and DP (+0.012) cultures.

Although cell death was the principal determinant of cell number in BB rat ATOC over time, the majority of recovered cells were nonetheless viable as determined by trypan blue exclusion. Representative examples of the morphology of day 8 DR-BB rat thymus cultures are shown in Fig. 2. Overall, the cultured fragments lack the anatomical characteristics of normal in vivo thymus, but contain large numbers of viable lymphoid and thymic stromal cells (Fig. 2*A*). At higher magnification (Fig. 2*B*), viable mononuclear cells appear to predominate, and thymic stromal cells can also be identified. However, examination of individual cell types in selected fields did reveal morphologic evidence of cell death by apoptosis (Fig. 2*C*). Macrophages could be identified in areas of cultured fragments that contain ingested cells with condensed nuclear chromatin and apoptotic bodies.

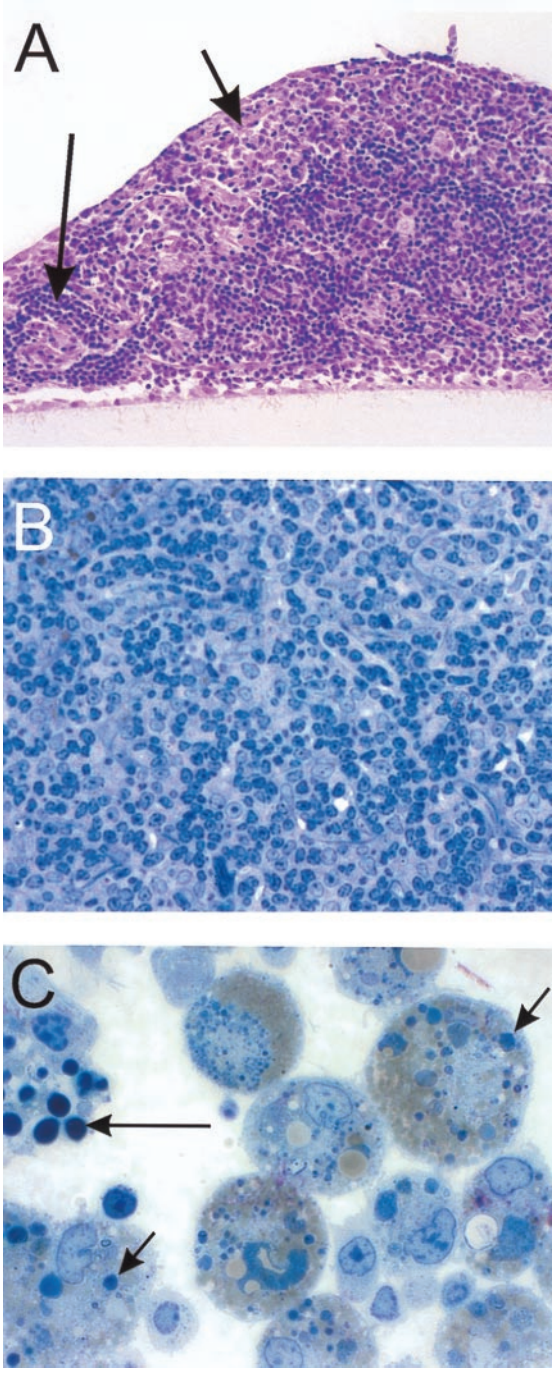

FIGURE 2. Representative histological specimens obtained from day 8 cultures of adult DR-BB rat thymi. *A*, Cross section of an intact thymic fragment stained with hematoxylin and eosin. The membrane on which the fragment was cultured is at the bottom. Viable lymphoid (long arrow) and stromal (short arrow) cells are abundant (magnification, ×20). *B*, Thin section of an intact thymic fragment stained with toluidine blue. Small lymphocytes are predominant, and lighter-stained stromal cells are present (magnification, ×40). *C*, Higher-power view of a thin section of a thymic fragment stained with toluidine blue. The field shown was at the edge of a fragment where macrophages were most easily visualized. The small arrows identify characteristic apoptotic bodies of variable size. The long arrow identifies a macrophage with ingested apoptotic cells with condensed nuclei. Lipofuscin pigmentation can be seen in many of the macrophages (magnification, ×100).

Rates of cell proliferation and apoptosis in ATOC

Based on our kinetic analysis (Fig. 1), we next directly tested the hypothesis that differences in the rate of thymocyte apoptosis but not cell proliferation accounted for the differential recovery of DP and DR cells in ATOC. We examined the dynamics of cell proliferation by measuring the uptake of BrdU. We also assessed the

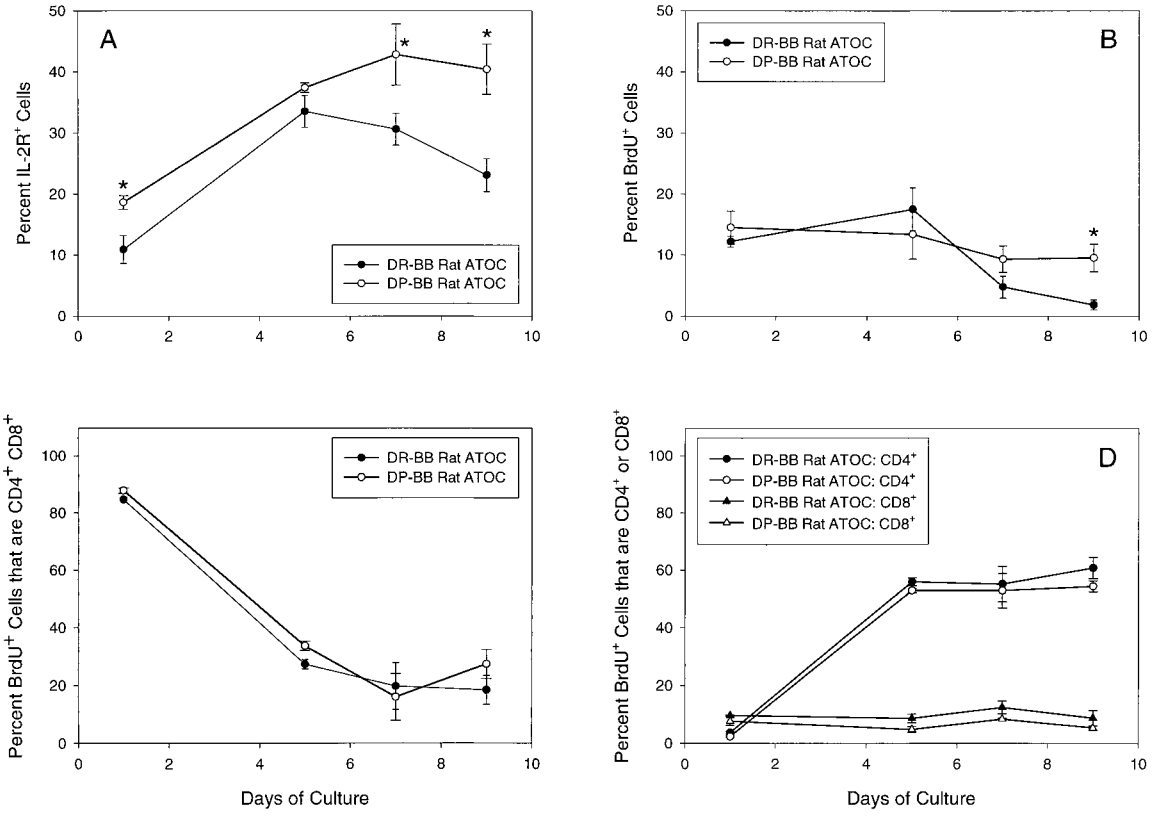

FIGURE 3. Percentage of viable cells recovered from DR- and DP-BB rat ATOC at different time points. Overall percentages of IL-2Rα^+ and BrdU$^+$ cells are shown in *A* and *B*, respectively. The fraction of BrdU$^+$ cells that were also CD4$^+$CD8$^+$ is shown in *C*. The fractions of BrdU$^+$ cells that were CD4$^+$ and CD8$^+$ are shown in *D*. Cells were recovered from DR- and DP-BB rat ATOC at the time points indicated. Results are presented as the mean ± 1 SD of three or four cultured thymus lobes. ∗, $p < 0.03$ *vs* DR-BB rat ATOC. No other paired comparisons of DP- vs DR-BB rat ATOC were statistically significant.

activation state of cells in ATOC by measuring the surface expression of IL-2R α-chain.

Few IL-2R$^+$ cells were detected in fresh thymocyte preparations (data not shown) or on day 1 of culture (Fig. 3*A*). The percentage of IL-2R$^+$ cells thereafter increased to about 30% on day 5 in both DR- and DP-BB rat ATOC. The percentage of IL-2R$^+$ cells remained at this level in DP-BB ATOC through day 9, but declined somewhat in DR-BB rat ATOC. Consistent with reports that a high frequency of T cells in DP rats have characteristics of activated T cells (29–33), we observed that the percentage of activated IL-2R$^+$ cells was statistically significantly greater in DP- than in DR-BB rat ATOC at three of the four time points sampled.

The overall percentage of BrdU$^+$-proliferating cells in ATOC was similar to the percentage of activated IL-2R$^+$ cells on day 1 of culture (~10–15%, Fig. 3*B*). However, over time the percentage of BrdU$^+$ cells did not increase, and in the case of DR-BB rat ATOC actually declined. By day 9 of culture, the percentage of BrdU$^+$ cells was significantly greater in DP- than in DR-BB rat ATOC (Fig. 3*B*).

We next measured the number of TUNEL$^+$ cells present in ATOC. In the first experiment (Fig. 4*A*), all nucleated cells were analyzed, and the data set therefore includes viable cells, cells in the process of apoptosis, and dead cells. Consistent with previous observations (34), the overall percentage of TUNEL$^+$ apoptotic cells was very low in freshly isolated DR- (1.4 ± 0.6%) and DP-BB (1.6 ± 0.8%) thymocytes (Fig. 4*A*). The percentage of TUNEL$^+$ cells then increased and remained elevated throughout the duration of the study. As predicted by the kinetic model shown in Fig. 1, the percentage of TUNEL$^+$ cells was statistically significantly greater in DP than in DR-BB thymocyte cultures at all time points after day 2.

ATOC of DR- and DP-BB rat thymus yield similar percentages of TCR-$\alpha\beta^{high}$ and CD4 single-positive, but not CD8 single-positive, T cells over time

To characterize the physiology of rat ATOC, cell subsets present in both freshly isolated and cultured DR and DP thymi were identified by flow cytometry using single labeling for TCR-$\alpha\beta$ and dual labeling for CD4 and CD8. Fig. 5 shows phenotypic analyses of percentages of CD4 CD8 double-positive, TCR-$\alpha\beta^{high}$, CD4 single-positive, and CD8 single-positive cells over time. The percentage of immature CD4$^+$ CD8$^+$ cells in freshly isolated DP- and DR-BB thymocytes was ~80%; this percentage declined progressively to ~5% during culture (Fig. 5*A*). The percentage of double-positive cells in DP and DR ATOC remained similar throughout the period of observation.

In both DR- and DP-BB ATOC, the decline in the percentage of immature double-positive cells was accompanied by a progressive increase in the percentage of mature TCR-$\alpha\beta^{high}$ and CD4 single-positive cells (Fig. 5, *B* and *C*). The percentages of TCR-$\alpha\beta^{high}$ cells in freshly isolated DR- and DP-BB thymocytes were 19.0 ± 2.5% and 15.6 ± 1.6%, respectively. These values increased to 93.6 ± 0.8% and 91.2 ± 1.8% on day 11. CD4 single-positive cells increased in freshly isolated DR- and DP-BB thymocytes from 11.4 ± 0.9% and 9.8 ± 1.8%, respectively, on day 0 to 68.0 ± 2.4% and 72.9 ± 2.3% on day 11. Again, the percentages

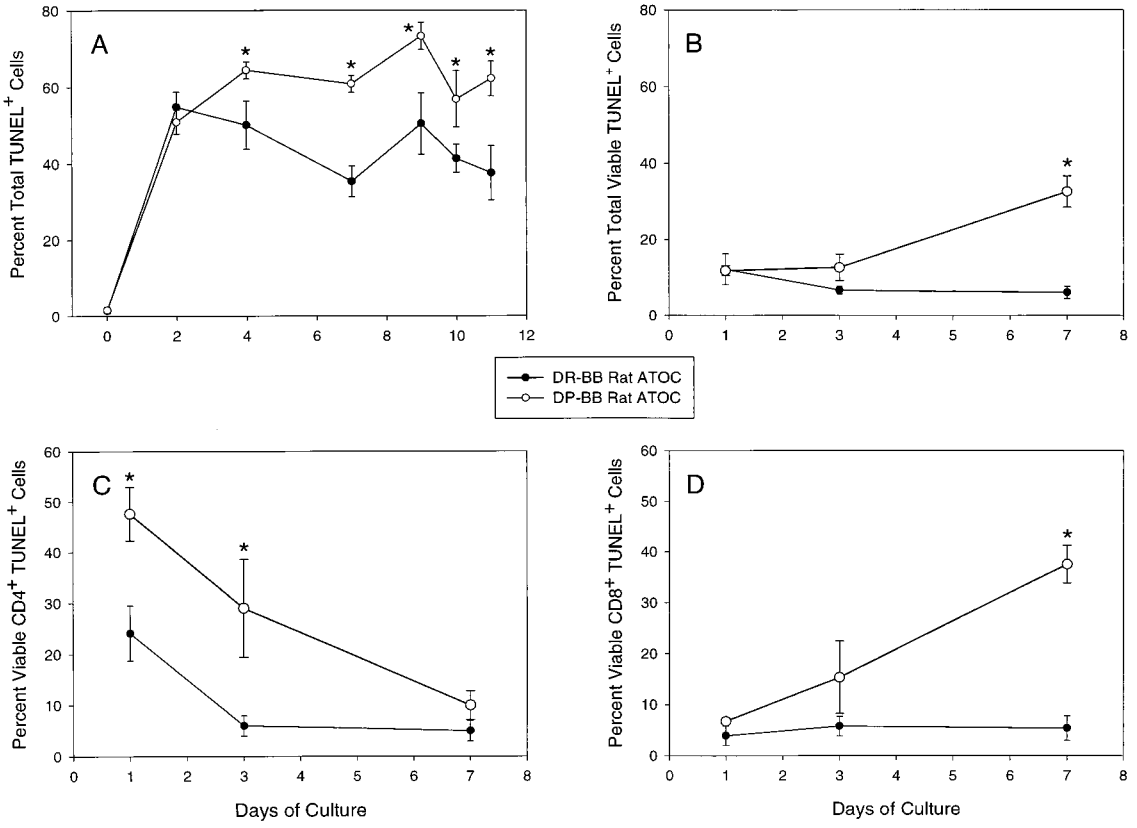

FIGURE 4. Percentages of TUNEL$^+$ cells recovered from DR- and DP-BB rat ATOC over time. *A*, Percentage of total TUNEL$^+$ cells, including viable, dying, and dead cells but excluding erythrocytes. *B*, Percentage of total viable TUNEL$^+$ cells. *C*, Percentage of viable CD4 single-positive cells that were also TUNEL$^+$. *D*, Percentage of viable CD8 single-positive cells that were also TUNEL$^+$. Results are presented as the mean ± 1 SD of four cultured thymus lobes or, for the day 0 time point in *A*, 11–12 uncultured thymus lobes. ∗, $p < 0.025$ vs DR-BB rat ATOC. No other paired comparisons of DP- vs DR-BB rat ATOC were statistically significant.

observed in DP- and DR-BB rat ATOC were similar throughout the period of observation.

In contrast, the percentages of CD8 single-positive cells in DP and DR cultures exhibited different patterns. The percentage of CD8$^+$ cells in freshly isolated thymocytes was higher in DR- (6.2 ± 1.4%) than in DP-BB (3.9 ± 0.7%) rat ATOC (Fig. 5*D*). This relatively small difference persisted during the first 6 days of ATOC; by day 6, the percentage of CD8$^+$ DR cells had risen to 23.5 ± 0.8% and the percentage of CD8$^+$ DP cells had risen to 20.0 ± 1.2%. Subsequently, however, the percentage of CD8$^+$ DR cells remained stable whereas the percentage of CD8$^+$ DP cells declined sharply. By day 11, the percentage of CD8$^+$ DR cells was still 20.6 ± 3.6%, whereas the percentage of CD8$^+$ DP cells had fallen to 8.2 ± 1.2% ($p < 0.001$). The CD4:CD8 ratio on day 7 of ATOC was 2.5:1 for DR and 3.9:1 for DP rats. By day 11, CD4: CD8 ratios were still more divergent, 3.3:1 and 9.1:1 for DR and DP cultures, respectively.

To determine whether the divergence of CD4:CD8 ratios for DR and DP cultures at later time points was due to differences in proliferation, we measured the percentage of BrdU$^+$-proliferating cells that were CD4$^+$, CD8$^+$, and double positive (Fig. 3, *C* and *D*). In each case, the percentages were statistically similar for DR- and DP-BB rat ATOC. As expected, the number of BrdU$^+$-proliferating double-positive cells declined over time (Fig. 3*C*), whereas the percentage of BrdU$^+$-proliferating CD4$^+$ cells increased over time (Fig. 3*D*). In contrast, the percentage of BrdU$^+$-proliferating CD8$^+$ cells remained low and constant over time (Fig. 3*D*).

Given the absence of differences in proliferation, we next asked if the divergence of CD4:CD8 ratios for DR and DP cultures at later time points was due to differences in rates of cell death. To do so, we measured the percentage of TUNEL$^+$ cells that were CD4$^+$, CD8$^+$, and double positive (Fig. 4, *B–D*). In these experiments, only viable cells were analyzed so as to include only those cells in the process of apoptosis. This gating also permitted us to compare the relative rates of apoptosis in DR- and DP-BB rat ATOC. We observed that percentages of TUNEL$^+$ but viable cells were initially similar in DR- and DP-BB rat ATOC but subsequently was much higher in the DP cultures (Fig. 4*B*). This result is consistent with the data obtained when all nucleated cells were analyzed (Fig. 4*A*). Subset analysis disclosed additional differences. The percentage of CD4$^+$ TUNEL$^+$ cells was initially higher in DP- than in DR-BB rat ATOC, but the percentages were similarly low by day 7 of culture (Fig. 4*C*). In contrast, the percentage of CD8$^+$ TUNEL$^+$ cells was initially similar and low in DP- and DR-BB rat ATOC, but the percentage subsequently became much higher in the DP cultures (Fig. 4*D*).

The percentages of Thy1.1$^+$ immature T cells decline at comparable rates in DP- and DR-BB rat ATOC

To analyze further the maturation of T cells in ATOC, we next measured the expression of the differentiation antigen Thy 1.1. Thy 1.1 expression declines as rat T cells mature (20, 22, 35). Virtually all rat thymocytes are Thy 1.1^{bright}; recent thymic emigrants are Thy 1.1^{low}; and peripheral T cells are Thy 1.1$^-$ (20, 22, 35). Fig. 6 (*upper panel*) shows that the percentages of Thy 1.1$^+$ cells in

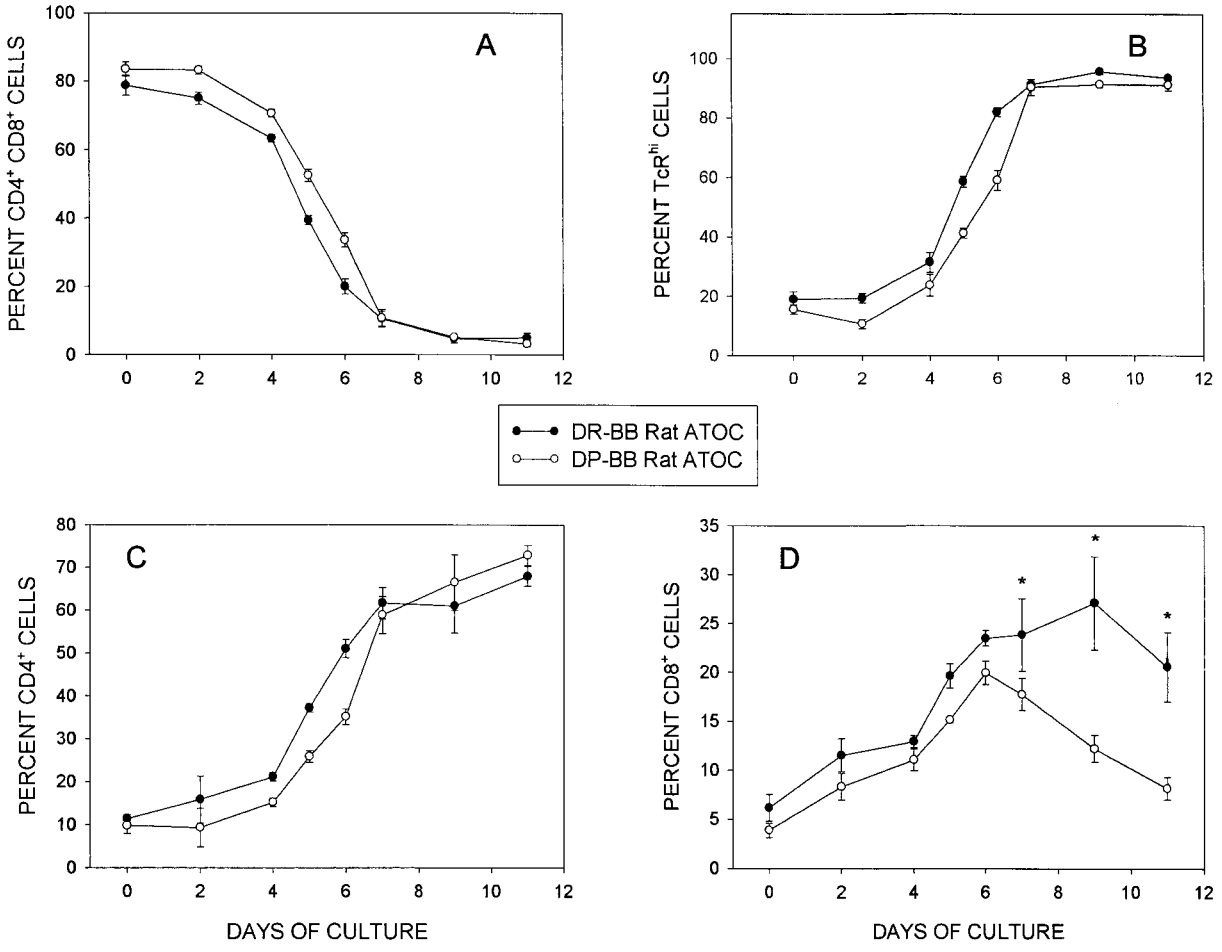

FIGURE 5. Percentages of CD4 CD8 double-positive (*A*), TCR-$\alpha\beta^{high}$ (*B*), CD4 single-positive (*C*), and CD8 single-positive (*D*) cells recovered from DR- and DP-BB rat ATOC over time. Results are expressed as the mean ± 1 SD of 4–10 cultured thymus lobes or, for the day 0 time point, 11–12 uncultured thymus lobes. *, $p < 0.001$ vs DP-BB at the corresponding time point.

both DR- and DP-BB rat ATOC were very similar over time. The percentage of Thy 1.1^+ cells declined from >95% in uncultured thymocytes to 12–13% on day 9. Thy 1.1 staining was very bright at early time points and progressively diminished in intensity with time, an observation that is consistent with progressive T cell maturation. Representative flow histograms for Thy 1.1 are shown in Fig. 7.

DP-BB rat thymocytes generate fewer RT6.1$^+$ mature T cells than do DR-BB rat thymocytes in ATOC

RT6.1 is an alloantigen that is expressed postthymically on mature $CD4^+$ and $CD8^+$ T cells and is severely deficient in the DP strain (11, 36, 37). Mature $RT6.1^+$ T cells, which are absent (<1%) in the thymus, develop in both DR- and DP-BB ATOC, reach maximal levels by day 7, and decline thereafter (Fig. 6, *lower panel*). The generation of substantial numbers of $RT6^+$ T cells in DP ATOC is striking given the near absence of these cells in the DP peripheral lymphoid tissues (3). However, in comparison with DR-BB rat ATOC, DP-BB rat ATOC generated a statistically significantly smaller percentage and number of $RT6^+$ cells than did DR-BB rat cultures. On day 7 of culture, 34.1 ± 1.7% of $CD4^+$ cells in DR-BB rat ATOC were $RT6.1^+$ ($8.1 \pm 1.1 \times 10^6$ cells). In contrast, 21.3 ± 12.3% of $CD4^+$ cells in DP-BB rat ATOC were $RT6.1^+$ ($1.4 \pm 0.8 \times 10^6$ cells). On day 7, 87.3 ± 0.6% of $CD8^+$ cells in DR-BB rat ATOC were $RT6.1^+$ ($20.9 \pm 2.5 \times 10^6$ cells). In contrast, 79.0 ± 6.6% of $CD8^+$ cells in DP-BB rat ATOC were $RT6.1^+$ ($6.0 \pm 0.7 \times 10^6$ cells). Representative flow histograms for RT6 are shown in Fig. 8. Both DR and DP cultures generate more Thy 1.1^{low} and $RT6.1^+$ cells than are present in freshly isolated thymi.

Addition of a caspase inhibitor increases the number of mature and immature T cells generated by DP-BB rat ATOC

Our observation of apoptotic cells in morphologic analyses (Fig. 2), and in TUNEL assays (Fig. 4), suggested that a major cell death pathway in rat ATOC is apoptosis. To test this hypothesis, DR- and DP-BB rat thymi were cultured in the presence or absence of the inhibitor of caspase-dependent apoptosis, Z-VAD-FMK, at various concentrations. Z-VAD-FMK is a general inhibitor of caspases with broader specificity than the tetra-peptide-based inhibitors YVAD and DEVD (38–40). Z-VAD-FMK was chosen for these experiments on the basis of recent reports documenting the involvement of caspases in negative selection (41, 42) and anti-CD3-mediated thymocyte apoptosis (40). Cultures were analyzed by flow cytometry for cell surface expression of CD4, CD8, and RT6.1.

As shown in Fig. 9, the number of $CD4^+CD8^+$, $RT6.1^+$, $CD4^+CD8^-$, and $CD4^-CD8^+$ cells recovered from DP-BB rat

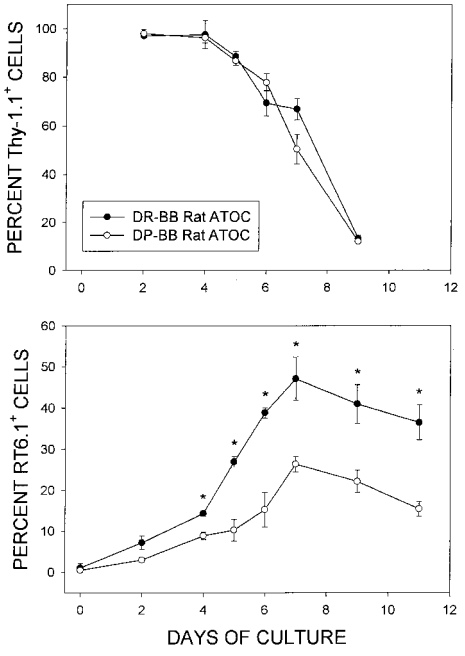

FIGURE 6. Percentage of cells expressing the differentiation Ags Thy1.1 (*upper panel*) and RT6.1 (*lower panel*) in DR- and DP-BB rat ATOC over time. Results are expressed as the mean ± 1 SD of 4–15 cultured thymus lobes or, for day 0, 10–11 uncultured thymus lobes. *, $p <$ 0.001 DP-BB at the corresponding time point.

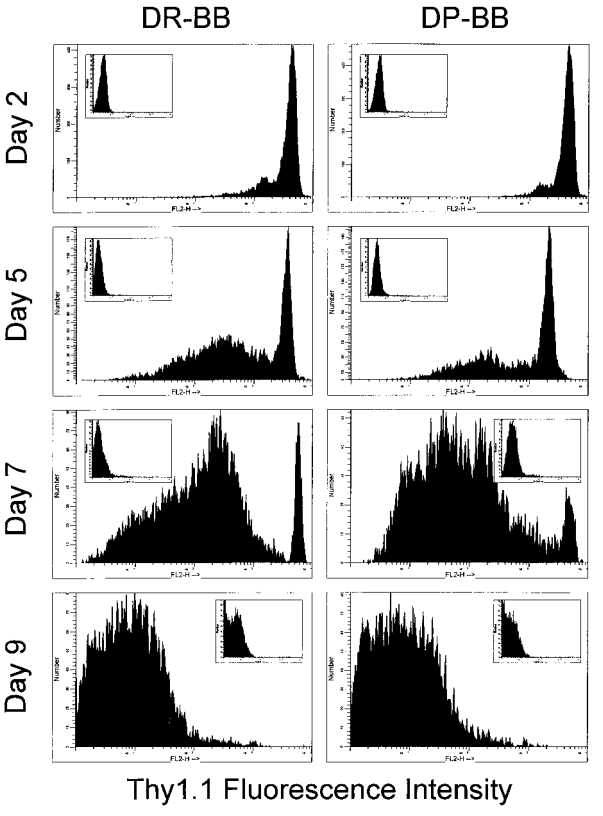

FIGURE 7. Surface density of Thy1.1 in DR and DP ATOC. Panels show representative flow cytometry profiles for DR (*left*) and DP (*right*) ATOC. In these histograms, cell number (vertical axis) is plotted against fluorescence intensity (horizontal axis). Background isotype control values are shown in the insets. The vertical axis scale varies for each histogram, but the vertical axes of each histogram and its control inset are the same in all cases.

thymi cultured for 7 days in the presence of Z-VAD-FMK increased in a dose-dependent manner. Compared with cultures performed in the absence of the inhibitor, the number of $CD4^+CD8^+$, $RT6.1^+$, $CD4^+CD8^-$, and $CD4^-CD8^+$ cells increased 11.0-, 6.5-, 2.5-, and 4.7-fold, respectively. Culture in the presence of Z-VAD-FMK also increased the number of immature $CD4^+CD8^+$ cells recovered from DR-BB rat ATOC by a factor of 2 at the highest concentrations, but Z-VAD-FMK had little or no effect on the number of mature $RT6.1^+$, $CD4^+CD8^-$, or $CD4^-CD8^+$ cells recovered.

Qualitatively similar results for both DR- and DP-BB rat ATOC were obtained in one additional experiment terminated on day 6. Compared with DP-BB rat thymus cultures performed in the absence of Z-VAD-FMK, the number of $CD4^+CD8^+$, $RT6.1^+$, $CD4^+CD8^-$, and $CD4^-CD8^+$ cells increased 6.3-, 3.7-, 2.0-, and 3.9-fold, respectively. Similarly, culture in the presence of Z-VAD-FMK also increased the number of immature $CD4^+CD8^+$ cells recovered from DR-BB rat ATOC by a factor of 2.1, but did not increase the recovery of mature cells.

Discussion

We report the development of a rat ATOC system and its application to the analysis of normal and abnormal T cell development. We demonstrate that cultures of thymi from phenotypically and physiologically normal DR-BB rats generate cells with mature peripheral T cell phenotypes, with the majority of nonmaturing cells undergoing apoptosis. In contrast, cultures of DP-BB rat thymi exhibit more extensive apoptosis and generate significantly fewer Thy 1.1^- $RT6^+$ mature T cells. These results demonstrate that ATOC recapitulates the normal and abnormal T cell development seen in vivo in these coisogenic animal models of human type 1 diabetes.

This recapitulation by ATOC exhibits remarkable fidelity to the in vivo physiology for both the DP and DR cultures. In vivo T cell development in the DR-BB rat generates normal numbers of T cells with a normal distribution of phenotypes (3, 11, 20). Ontogenetically, DR-BB T cell development requires 3–5 days of intrathymic processing during which ~3% of double-positive thymocytes survive selection and mature into single-positive thymocytes. These cells then migrate to the periphery where they acquire a mature phenotype by down-regulating the expression of Thy 1.1 and acquiring the expression of RT6 within 3–5 days (20, 22, 35). Each of these kinetic and phenotypic features of normal DR T cell development was reflected in DR rat ATOC.

The abnormal development of T cells in DP-BB rats also appears to begin intrathymically; it is intrinsic to the DP-BB rat stem cell and not to any defect in the DP thymus or peripheral lymphoid compartment (43). Although subtle defects in DP-BB rat T cells may be detectable at the double-positive stage of thymocyte development, abnormal differentiation first becomes readily detectable at the single-positive stage, at which time there is a major deficiency in $CD8^+$ TCR^{high} positively selected thymocytes (19). Thereafter, there is also reduced export of T cells from the thymus (20, 22) and a failure of recent thymic emigrants to differentiate into Thy 1.1^- $RT6^+$ mature T cells (20, 22). These cells, which appear to be activated (29–33), undergo apoptosis and are removed by the liver (21). Recapitulating the in vivo intrathymic physiology, DP-BB ATOC was characterized by increased expression of the activation IL-2Rα marker, increased apoptosis, deficiencies in markers of T cell maturation, and reduced overall cell output.

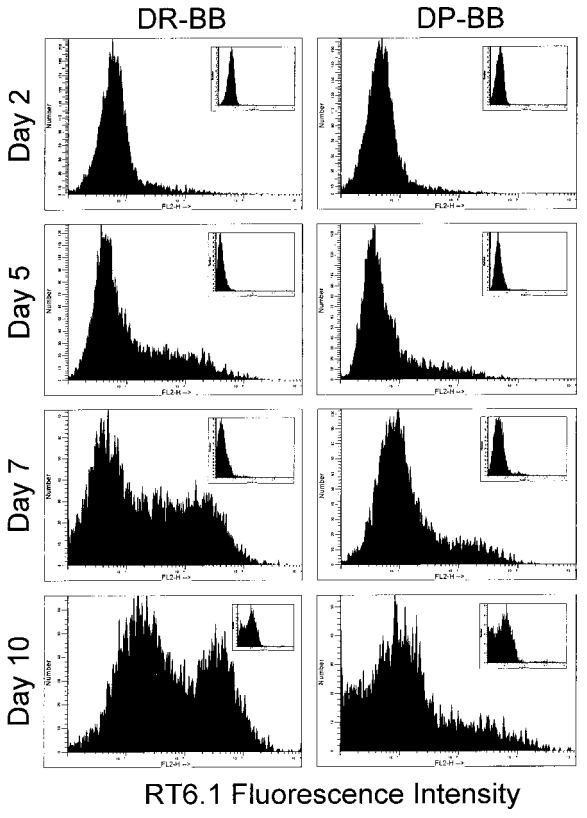

FIGURE 8. Surface density of RT6.1 in DR and DP ATOC. Representative flow cytometry profiles are shown for DR (*left*) and DP (*right*) ATOC. In these histograms, cell number (vertical axis) is plotted against fluorescence intensity (horizontal axis). Background isotype control values are shown in the insets. The vertical axis scale varies for each histogram, but the vertical axes of each histogram and its control inset are the same in all cases.

In general, rat ATOC is characterized by progressive cell maturation in the context of extensive cell death. A rapid decline in cell number was observed with both DR- and DP-BB rat cultures. About half of all cells present on day 2 of culture were TUNEL$^+$, either dead or dying of apoptosis. This extensive degree of cell death is consistent with the fact that, in normal rat thymus, >97% of cells fail to mature and emigrate to peripheral tissues (44). In addition, as expected from in vivo studies, the decline in cell number observed in DP-BB ATOC was even greater than that observed with DR rat thymi. Because thymi in ATOC cannot be reseeded with immature bone marrow-derived progenitors, the number of cells recoverable over time declines. The decline is exponential, indicating that the number of cells present over time is principally a function of the number of cells present earlier, consistent with randomly occurring cell death.

The dramatic loss of cells seen during the first 5 days of culture is consistent with the in vivo life span of cells that fail to undergo positive selection (44–46). We interpret the loss of cells over time in ATOC as due to programmed cell death. This interpretation is supported by our observation that the percentage of TUNEL$^+$ cells is initially low, then increases, and finally plateaus. The presence of apoptotic cells was also confirmed histologically by the observation of apoptotic bodies within phagocytes.

It could be argued that the decline in cell number is due to trauma leading to cell death by necrosis, and we cannot exclude the possibility that some degree of tissue injury occurs during the processing of thymi for culture. However, cell death due to necrosis would be expected to result in the accumulation of cellular debris in the cultures. This was not seen. In addition, we observed proliferation of maturing thymocytes over time. The number of proliferating thymocytes as judged by the percentage of BrdU$^+$ cells was statistically similar in both DP- and DR-BB ATOC at most time points. The only exception was a modestly but significantly higher rate of proliferation in DP-BB rat ATOC on day 9. We conclude that DR rat ATOC recapitulates the development of normal T cell numbers observed in the periphery of these animals in vivo. In contrast, DP-BB ATOC recapitulates the development of lymphopenia that is characteristic of these animals due to homozygosity for the *lyp* locus (12).

DR- and DP-BB rat ATOC recapitulates not only differences in T cell production, but also strain-specific differences in cell phenotype. Culture of DR-BB rat thymi generates mature CD4 and CD8 single-positive cells with up-regulated TCRs. DR-BB rat cultures also generate mature T cells that down-regulate Thy1.1 and eventually up-regulate RT6. In contrast, DP-BB rat cultures generate smaller numbers and smaller percentages of CD8 single-positive cells than do DR cultures. Like DR-BB rat ATOC, DP-BB cultures initially appear to generate Thy1.1$^-$ RT6$^+$ cells, but over time DP cultures yield fewer mature RT6$^+$ cells than do DR cultures. DP-BB rat ATOC does generate a percentage of CD4$^+$ cells that is similar to that observed in DR-BB rat cultures, but due to the overall decreased cellularity of DP cultures, the number of CD4$^+$ cells generated is less. It is likely that these maturing cells are lost due to apoptosis, and it would appear that the process recapitulates the in vivo loss of maturing T cells in the DP rat that occurs by apoptosis in the liver (21).

We hypothesize that the severe deficiency in single-positive cells in DP-BB rats in vivo and in DP-BB rat ATOC in vitro is the result of the failure of double positive thymocytes to be rescued from apoptosis during successful positive selection. This hypothesis in turn predicts that inhibition of apoptosis in DP-BB rat thymi should 1) increase the number of immature double-positive thymocytes and 2) permit their subsequent differentiation into mature single-positive thymocytes. These predictions were confirmed by our observation of increased DP-BB rat cell recoveries in thymus cultures conducted in the presence of the caspase inhibitor Z-VAD-FMK. The increase was greatest for double-positive cells, but recovery of RT6$^+$, CD8$^+$, and CD4$^+$ cells was also enhanced. On the basis of these data, we speculate that the function of the *lyp* gene, which is responsible for the lymphopenia of the DP-BB rat (12), is to enhance caspase-mediated apoptosis in thymocytes that have successfully undergone positive selection. However, we recognize that these observations may be interpreted in many other ways. Z-VAD-FMK blocks apoptosis initiated by many processes. It is possible that cell death in developing thymocytes in DP-BB rat ATOC is the result of failure to receive or respond to cytokine or stromal cell signals. Alternatively, it may represent increased negative selection or neglect. It is difficult to distinguish among these alternatives in a nontransgenic system.

We observed that the effect of Z-VAD-FMK on DR-BB rat ATOC was much smaller in magnitude than its effect on DP ATOC. DR-BB rats are nonlymphopenic and wild type at the *lyp* locus (3, 12). Because positive selection of thymocytes in DR-BB rats appears to be normal, it would be predicted that Z-VAD-FMK would not influence the yield of mature T cells generated by DR rat ATOC. This prediction was confirmed. We attribute the modest increase in the yield of double-positive cells generated by DR rat ATOC in the presence of Z-VAD-FMK to the reported general activity of caspases in thymocyte selection (41, 42).

The development of rat ATOC that recapitulate in vivo events holds promise for enhancing our understanding of the processes

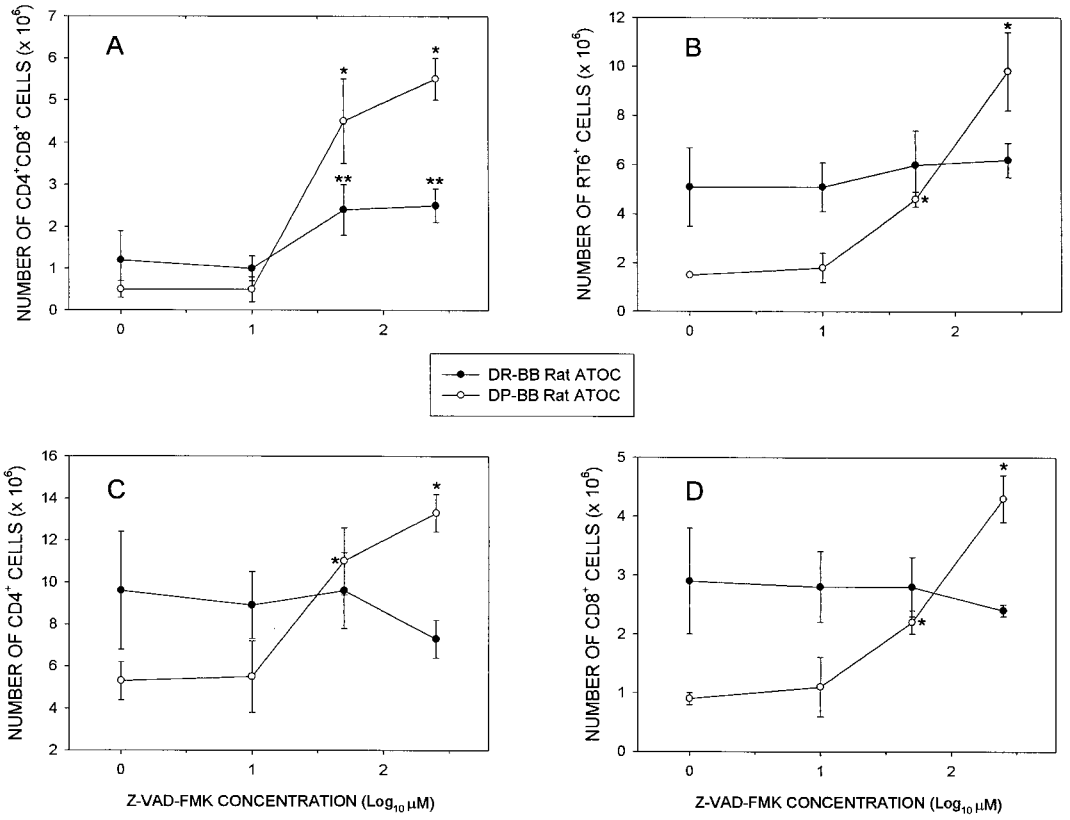

FIGURE 9. Mean number of lymphocytes recovered on day 7 from DR- and DP-BB rat thymi cultured in the presence or absence of varying doses of the general caspase inhibitor Z-VAD-FMK added on day 0. The number of $CD4^+CD8^+$ (*A*), $RT6.1^+$ (*B*), $CD4^+CD8^-$ (*C*), and $CD4^-CD8^+$ cells (*D*) is plotted as a function of inhibitor concentration. Cell number was calculated by counting the total number of viable cells present at the end of the culture period and multiplying by the subset percentage as determined by flow microfluorometry (see *Materials and Methods*). Shown is a single representative experiment. Each data point represents the mean ± 1 SD of three individual half-thymus lobes. Statistical comparisons were made within strain only. Overall analysis of variance revealed statistically significant differences at the $p < 0.001$ level for each phenotype in the DP-BB cultures. In the case of the DR-BB cultures, statistically significant differences were observed only for the $CD4^+CD8^+$ phenotype ($p < 0.025$). *, $p < 0.005$ vs no inhibitor; **, $p < 0.025$ vs no inhibitor.

that lead to the generation of autoreactivity in the rat. Like previously described rodent fetal thymus organ cultures (FTOC), rat ATOC allows for analysis of T cell development in the absence of seeding of the thymus with thymocyte progenitors and in the absence of emigration from the thymus. However, compared with FTOC the development of rat ATOC offers several advantages. Whereas FTOC generates predominantly CD8 single-positive cells, ATOC applied to a phenotypically normal animal like the DR-BB rat generates cells with a normal CD4:CD8 ratio. Applied to the lymphopenic DP-BB rat, ATOC recapitulates defective T cell development. These characteristics suggest that ATOC reflects both normal and abnormal T cell development with reasonable fidelity. In addition, ATOC is technically simpler than FTOC in that it generates larger numbers of cells without requiring timed pregnancies or microdissection of the thymus. Another potential advantage of ATOC over FTOC for the study of autoimmunity may derive from the fact that fetal and adult thymocytes may not be functionally identical (25, 47, 48). Rat ATOC also differs from suspension cultures of thymocytes in that the three-dimensional structure of the thymic microenvironment is disrupted in suspension, and the cells generated in suspension cultures do not develop normally (49, 50).

The availability of ATOC provides the opportunity to analyze in detail the earliest processes that lead to the generation of autoreactive cells. Our laboratory has demonstrated, for example, that autoreactive cells in the BB rat are generated intrathymically. Thymocytes from 8-wk-old DR-BB rats are capable of the adoptive transfer of IDDM (25). However, the mechanisms underlying this observation are difficult to identify and modify in vivo. ATOC should permit investigators to circumvent this problem. In preliminary studies we have observed that cells obtained from day 7 DR-BB rat ATOC transfer diabetes to histocompatible athymic recipients (B.J.W., unpublished observations). ATOC will also permit detailed analysis of the early events that result in enhanced apoptosis in the DP-BB rat and may lead to further insights into the function of the *lyp* locus (12, 51). Studies to modify the development of autoreactive thymocytes in ATOC by strategies including cytokine polarization, exposure to candidate autoantigens, and coculture with regulatory cells are underway in our laboratory.

Acknowledgments

We thank Dr. Bruce Woda for consultation on the histological analyses, Roger Solomon for preparation of the thin sections, Kelly Lake for technical assistance, and Patricia Raymond for secretarial assistance.

References

1. Mordes, J. P., D. L. Greiner, and A. A. Rossini. 1996. Animal models of autoimmune diabetes mellitus. In *Diabetes Mellitus. A Fundamental and Clinical Text*. D. LeRoith, S. I. Taylor, and J. M. Olefsky, eds. Lippincott-Raven, Philadelphia, p. 349.

2. Rossini, A. A., J. P. Mordes, E. S. Handler, and D. L. Greiner. 1995. Human autoimmune diabetes mellitus: lessons from BB rats and NOD mice—caveat emptor. *Clin. Immunol. Immunopathol. 74:2.*
3. Crisá, L., J. P. Mordes, and A. A. Rossini. 1992. Autoimmune diabetes mellitus in the BB rat. *Diabetes Metab. Rev. 8:9.*
4. Guberski, D. L. 1994. Diabetes-prone and diabetes-resistant BB rats: animal models of spontaneous and virally induced diabetes mellitus, lymphocytic thyroiditis, and collagen-induced arthritis. *ILAR News 35:29.*
5. Jackson, R., N. Rassi, T. Crump, B. Haynes, and G. S. Eisenbarth. 1981. The BB diabetic rat: profound T-cell lymphocytopenia. *Diabetes 30:887.*
6. Poussier, P., A. F. Nakhooda, A. A. F. Sima, and E. B. Marliss. 1981. Lymphopenia in the spontaneously diabetic "BB" Wistar rat. *Diabetologia 21:317.*
7. Bellgrau, D., A. Naji, W. K. Silvers, J. F. Markmann, and C. F. Barker. 1982. Spontaneous diabetes in BB rats—evidence for a T-cell dependent immune response defect. *Diabetologia 23:359.*
8. Elder, M. E., and N. K. Maclaren. 1983. Identification of profound peripheral T lymphocyte immunodeficiencies in the spontaneously diabetic BB rat. *J. Immunol. 130:1723.*
9. Guttmann, R. D., E. Colle, F. Michel, and T. Seemayer. 1983. Spontaneous diabetes mellitus in the rat. II. T lymphopenia and its association with clinical disease and pancreatic lymphocytic infiltration. *J. Immunol. 130:1732.*
10. Woda, B. A., A. A. Like, C. Padden, and M. McFadden. 1986. Deficiency of phenotypic cytotoxic-suppressor T lymphocytes in the BB/W rat. *J. Immunol. 136:856.*
11. Greiner, D. L., E. S. Handler, K. Nakano, J. P. Mordes, and A. A. Rossini. 1986. Absence of the RT-6 T cell subset in diabetes-prone BB/W rats. *J. Immunol. 136:148.*
12. Jacob, H. J., A. Pettersson, D. Wilson, Y. Mao, Å. Lernmark, and E. S. Lander. 1992. Genetic dissection of autoimmune type I diabetes in the BB rat. *Nat. Genet. 2:56.*
13. Guberski, D. L., L. Butler, W. Kastern, and A. A. Like. 1989. Genetic studies in inbred BB/Wor rats: analysis of progeny produced by crossing lymphopenic diabetes-prone rats with nonlymphopenic diabetic rats. *Diabetes 38:887.*
14. Markholst, H., S. Eastman, D. Wilson, B. E. Andreasen, and Å. Lernmark. 1991. Diabetes segregates as a single locus in crosses between inbred BB rats prone or resistant to diabetes. *J. Exp. Med. 174:297.*
15. Like, A. A., D. L. Guberski, and L. Butler. 1986. Diabetic BioBreeding/Worcester (BB/Wor) rats need not be lymphopenic. *J. Immunol. 136:3254.*
16. Colle, E. 1990. Genetic susceptibility to the development of spontaneous insulin-dependent diabetes mellitus in the rat. *Clin. Immunol. Immunopathol. 57:1.*
17. Martin, A.-M., E. P. Blankenhorn, M. N. Maxson, M. Zhao, J. Leif, J. P. Mordes, and D. L. Greiner. 1999. Non-MHC-linked diabetes susceptibility loci on chromosomes 4 and 13 in a backcross of the diabetes-prone BB/Wor rat to the Wistar Furth rat. *Diabetes. 48:50.*
18. Fuks, A., E. Colle, S. Ono, G. J. Prud'homme, T. Seemayer, and R. D. Guttmann. 1988. Immunogenetic studies of insulin-dependent diabetes in the BB rat. In *Frontiers in Diabetes Research: Lesson from Animal Diabetes II.* E. Shafrir and A. E. Renold, eds. John Libbey, London, p. 29.
19. Plamondon, C., V. Kottis, C. Brideau, M.-D. Métroz-Dayer, and P. Poussier. 1990. Abnormal thymocyte maturation in spontaneously diabetic BB rats involves the deletion of $CD4^{-}8^{+}$ cells. *J. Immunol. 144:923.*
20. Groen, H., F. A. Klatter, N. H. C. Brons, G. Mesander, P. Nieuwenhuis, and J. Kampinga. 1996. Abnormal thymocyte subset distribution and differential reduction of $CD4^{+}$ and $CD8^{+}$ T cell subsets during peripheral maturation in diabetes-prone BioBreeding rats. *J. Immunol. 156:1269.*
21. Iwakoshi, N. N., I. Goldschneider, F. Tausche, J. P. Mordes, A. A. Rossini, and D. L. Greiner. 1998. High frequency apoptosis of recent thymic emigrants in the liver of lymphopenic diabetes prone BioBreeding rats. *J. Immunol. 160:5838.*
22. Zadeh, H. H., D. L. Greiner, D. Y. Wu, F. Tausche, and I. Goldschneider. 1996. Abnormalities in the export and fate of recent thymic emigrants in diabetes-prone BB/W rats. *Autoimmunity 24:35.*
23. Fangmann, J., R. Schwinzer, H.-J. Hedrich, I. Klöting, and K. Wonigeit. 1991. Diabetes-prone BB rats express the RT6 alloantigen on intestinal intraepithelial lymphocytes. *Eur. J. Immunol. 21:2011.*
24. Waite, D. J., M. C. Appel, E. S. Handler, J. P. Mordes, A. A. Rossini, and D. L. Greiner. 1996. Ontogeny and immunohistochemical localization of thymus dependent and thymus independent $RT6^{+}$ cells in the rat. *Am. J. Pathol. 148:2043.*
25. Whalen, B. J., A. A. Rossini, J. P. Mordes, and D. L. Greiner. 1995. DR-BB rat thymus contains thymocyte populations predisposed to autoreactivity. *Diabetes 44:963.*
26. Tough, D. F., and J. Sprent. 1996. Measurement of T and B cell turnover with bromodeoxyuridine. In *Current Protocols in Immunology.* J. E. Coligan, A. M. Kruisbeek, D. H. Margulies, E. M. Shevach, and W. Strober, eds. John Wiley & Sons, New York, p. 4.7.1.
27. Nie, N. H., C. H. Hull, J. G. Jenkins, K. Steinbrenner, and D. H. Bent. 1975. *Statistical Package for the Social Sciences.* McGraw-Hill, New York, p. 1.
28. O'Brien, P. C., and M. A. Shampo. 1988. Statistical considerations for performing multiple comparisons in a single experiment. II. Comparisons among multiple therapies. *Mayo Clin. Proc. 63:816.*
29. Francfort, J. W., A. Naji, D. P. Markmann, W. K. Silvers, and C. F. Barker. 1985. "Activated" T-lymphocyte levels in the spontaneously diabetic BB rat syndrome. *Surgery 98:251.*
30. Field, C. J., R. Chayoth, M. Montambault, and E. B. Marliss. 1991. Enhanced 2-deoxy-D-glucose uptake and metabolism in splenocytes from diabetic and diabetes-prone BB rats: further evidence to support prior in vivo activation. *J. Biol. Chem. 266:3675.*
31. Francfort, J. W., C. F. Barker, H. Kimura, W. K. Silvers, M. Frohman, and A. Naji. 1985. Increased incidence of Ia antigen-bearing T lymphocytes in the spontaneously diabetic BB rat. *J. Immunol. 134:1577.*
32. Wu, G., C. J. Field, and E. B. Marliss. 1991. Elevated glutamine metabolism in splenocytes from spontaneously diabetic BB rats. *Biochem. J. 274:49.*
33. Groen, H., J. M. Pater, P. Nieuwenhuis, and J. Rozing. 1997. Elevated intracellular glutathione levels in $CD4^{+}$ T cells of BB rats. *Transplant. Proc. 29:1679.*
34. Surh, C. D., and J. Sprent. 1994. T-cell apoptosis detected in situ during positive and negative selection in the thymus. *Nature 372:100.*
35. Hosseinzadeh, H., and I. Goldschneider. 1993. Recent thymic emigrants in the rat express a unique antigenic phenotype and undergo post-thymic maturation in peripheral lymphoid tissues. *J. Immunol. 150:1670.*
36. Mojcik, C. F., D. L. Greiner, E. S. Medlock, K. L. Komschlies, and I. Goldschneider. 1988. Characterization of RT6 bearing rat lymphocytes. I. Ontogeny of the $RT6^{+}$ subset. *Cell. Immunol. 114:336.*
37. Mojcik, C. F., D. L. Greiner, and I. Goldschneider. 1991. Characterization of RT6-bearing lymphocytes. II. Developmental relationships of $RT6^{-}$ and $RT6^{+}$ T cells. *Dev. Immunol. 1:191.*
38. Shaw, E. 1990. Cysteinyl proteinases and their selective inactivation. *Adv. Enzymol. Relat. Areas Mol. Biol. 63:271.*
39. Nicholson, D. W., A. Ali, N. A. Thornberry, J. P. Vaillancourt, C. K. Ding, Gallant, Y. Gareau, P. R. Griffin, M. Labelle, and Y. A. Lazebnik. 1995. Identification and inhibition of the ICE/CED-3 protease necessary for mammalian apoptosis. *Nature 376:37.*
40. Sarin, A., M. L. Wu, and P. A. Henkart. 1996. Different interleukin-1β converting enzyme (ICE) family protease requirements for the apoptotic death of T lymphocytes triggered by diverse stimuli. *J. Exp. Med. 184:2445.*
41. Alam, A., M. Y. Braun, F. Hartgers, S. Lesage, L. Cohen, P. Hugo, F. Denis, and R. P. Sekaly. 1997. Specific activation of the cysteine protease CPP32 during the negative selection of T cells in the thymus. *J. Exp. Med. 186:1503.*
42. Clayton, L. K., Y. Ghendler, E. Mizoguchi, R. J. Patch, T. D. Ocain, K. Orth, A. K. Bhan, V. M. Dixit, and E. L. Reinherz. 1997. T-cell receptor ligation by peptide/MHC induces activation of a caspase in immature thymocytes: the molecular basis of negative selection. *EMBO J. 16:2282.*
43. Angelillo, M., D. L. Greiner, J. P. Mordes, E. S. Handler, N. Nakamura, U. McKeever, and A. A. Rossini. 1988. Absence of $RT6^{+}$ T cells in diabetes-prone BioBreeding/Worcester rats is due to genetic and cell developmental defects. *J. Immunol. 141:4146.*
44. Shortman, K., and R. Scollay. 1994. Immunology. Death in the thymus. *Nature 372:44.*
45. Merkenschlager, M., D. Graf, M. Lovatt, U. Bommhardt, R. Zamoyska, and A. G. Fisher. 1997. How many thymocytes audition for selection. *J. Exp. Med. 186: 1149.*
46. Surh, C. D., and J. Sprent. 1994. T-cell apoptosis detected in situ during positive and negative selection in the thymus. *Nature 372:100.*
47. Jenkinson, E. J., and G. Anderson. 1994. Fetal thymic organ cultures. *Curr. Opin. Immunol. 6:293.*
48. Anderson, G., J. J. T. Owen, N. C. Moore, and E. J. Jenkinson. 1994. Characteristics of an in vitro system of thymocyte positive selection. *J. Immunol. 153: 1915.*
49. Moore, N. C., E. J. Jenkinson, and J. J. T. Owen. 1992. Effects of the thymic microenvironment on the response of thymocytes to stimulation. *Eur. J. Immunol. 22:2533.*
50. Porritt, H. E., K. L. Anderson, R. K. Suniara, E. J. Jenkinson, and J. J. T. Owen. 1998. Cellular interactions in the thymus regulate the protein kinase C signaling pathway. *Eur. J. Immunol. 28:1197.*
51. Bieg, S., C. Moller, T. Olsson, and A. Lernmark. 1997. The lymphopenia (*lyp*) gene controls the intrathymic cytokine ratio in congenic BioBreeding rats. *Diabetologia 40:786.*